JOURNAL OF APPLIED ELECTROCHEMISTRY 24 (1994) 316–320

Performance characteristics of a certain class of electrolysers

T. Z. FAHIDY

Department of Chemical Engineering, University of Waterloo, Waterloo, Ontario, N2L 3G1, Canada

R. E. SIODA

Institute of Industrial Organic Chemistry, ul Annopol 6, 03-236, Warszawa-Zerań, Poland

Received 16 March 1993; revised 15 August 1993

The performance properties of a continuous-flow electrolyser are analysed under plug-flow and parabolic-flow conditions. The duty of the electrolyser is to produce a species via anodic oxidation or cathodic reduction, upon which the product undergoes a first-order irreversible chemical decomposition (without net electron transfer). The effect of various parameters on electrolyser performance is also discussed.

List of symbols

a electrode area per unit electrode length

a_ϕ, a_ψ constants in Equation 9(e); Plug flow: $a_\phi = ak_m/A_c u$; $a_\psi = (A_c k_1 + ak_m)/A_c u$; parabolic flow: $a_\phi = ak_m R^2/2A_c u_m$; $a_\psi = (A_c k_1 + ak_m) R^2/2A_c u_m$

A_c cross-sectional area of the electrolyser

c_A concentration of the electrode-product species; c_A^s its value at the electrode surface: c_A^o its value in the inlet-to-electrolyte stream; $\hat{c}_A^o$ its sectional average value at a set axial position; $\bar{c}_A$ its average value over the electrolyser length; c_A^E its exit value in a plug-flow reactor

Ei symbol denoting the exponential integral

F Faraday constant

i current density; i_x its value at a set axial position; i_m its average value over the electrolyser length

k_1 specific rate of the chemical decomposition reaction of species A

k_m mean mass transfer coefficient

L length of the electrolyser

r radial distance

R radius of a (parabolic) flow channel

u linear velocity of the electrolyte; u_m its mean value (parabolic-flow)

x axial coordinate; $0 \leqslant x \leqslant L$

z valency.

Greek symbols

β lumped parameter: $\phi c_A^s/\psi c_a^o$

τ_m mean residence time

ϕ lumped parameter: $ak_m/A_c u$; plug flow: $u =$ const; parabolic flow: $\phi \equiv a_\phi/(R^2 + r^2)$

ψ lumped parameter: $\phi = k_1/u$; plug flow: $u =$ const; parabolic flow: $\psi = a_\psi/(R^2 + r^2)$

Abbreviations

EC electrochemical reaction followed by a chemical reaction

ECE electrochemical/chemical/electrochemical reaction sequence

1. Introduction

The mechanisms of EC and ECE-type reactions have been of steady interest in the electroorganic chemistry literature [e.g. 1–4]. Representative examples can be cited from pseudo-first order [5] and second order [6] EC catalytic reactions, and the EC_2/rev-irr reactions involving $A \rightarrow B$; $2B \rightarrow C$ reaction steps [7–14]. The intricate structure of more complex mechanisms has been well illustrated by several studies [e.g. 15–18]. Experimental verification of proposed (theoretical) reaction sequence structures has been seriously hindered by extremely short life expectancies of intermediate reaction products, but the relatively recent development of ultrafast cyclic voltammetry [19, 20] may prove useful in the numerical pursuit of kinetic information.

The application of flow-through (porous-electrode) electrochemical cells to reactions of this kind has been shown by several researchers [e.g. 21, 22]. The flow regime has been assumed to be laminar with a characteristic parabolic velocity distribution [23, 24] which affects mass transport behaviour and overall performance [25, 26] in single-step electron transfer processes. A similar treatment of FTPE cells in the case of EC and ECE-type reactions suffers from the paucity of quantitative kinetic data [27–30] and, in certain cases, from the complexity of the reaction paths.

The purpose of this paper is to present a perfor-

0021-891X 1994 Chapman & Hall

mance analysis of a particular EC reaction scheme consisting of an electronation or de-electronation reaction occurring at the appropriate electrode followed by an essentially first order irreversible chemical reaction. In choosing numerical values of process parameters for quantitative illustration, the relatively well-known electrolytic decomposition of DPA [9,10-diphenylanthracene] has been taken as a reference model [29–31], following a simplified scheme [32]

$$\mathrm{DPA} \longrightarrow \mathrm{DPA}^+ + \mathrm{e}^- \qquad (1a)$$

$$\mathrm{DPA}^+ \xrightarrow{\mathrm{H_2O}} \cdots \qquad (1b)$$

but the approach is *not* limited, in principle, to any specific chemical species. It can also be extended to more complex reaction schemes. The major utility of the model is in the design of EC flow-through reactors, i.e. in the selection of bed length and the mean residence time for a preset reactant-to-product conversion.

2. Theory

2.1. *General*

Consider a flow-through electrochemical reactor, where an oxidized form of a species is electronated to a reduced form at the cathode, or inversely, a reduced form of a species is de-electronated to an oxidized form at the anode. The product A of the electrode reaction has an electrode-surface concentration c_A^s, and its concentration in the bulk solution, c_A, is determined by three factors: (i) mass transport of species A from the electrode surface; (ii) the rate of its decomposition in the bulk via first-order irreversible chemical kinetics with rate constant k_1; (iii) the concentration of species A in the reactor inlet flow, c_A^o (it may, of course, be zero). A material balance written for species A over an infinitesimal control volume ($A_c dx$) yields the differential equation

$$\frac{dc_A}{dx} + \frac{k_1}{u} c_A - \frac{i_x a}{zFA_c u} = 0 \qquad (2)$$

for the variation of its concentration along the reactor bed, $0 \leqslant x \leqslant L$, if one-dimensional convection (in the flow direction) dominates over diffusion and dispersion, and migration effects are negligible. The local current density

$$i_x = zFk_x(c_A^s - c_A)|_x \qquad (3)$$

is determined by the local mass transfer coefficient, and the local mass transport driving force, i.e. its concentration profile from electrode surface to bulk. Since the $c_A(x)$ function is a-priori not known, Equation 2 could be solved rigorously only by a cumbersome iterative improvement of successively obtained concentration profiles. In a much less complicated, albeit approximate approach, k_x is replaced by k_m, i.e. its value averaged over the reactor length, and by considering the mean value of the current density

$$i_m = zFk_m(c_A^s - c_A) \qquad (4)$$

In this instance the analytical solution of Equation 2 may be expressed as

$$\frac{c_A}{c_A^s} = \epsilon^{-\psi x} + \frac{\phi}{\psi}\left(\frac{c_A^s}{c_A^o}\right)(1 - \epsilon^{-\psi x}) \qquad (5)$$

If the velocity distribution across the bed is non-uniform, ϕ and ψ are functions of the space coordinates transverse to the reactor axis. The solution implies that c_A^s is (at least approximately) constant; this assumption is well justified if the current is sufficiently large to maintain the surface concentration of species A near its solubility limit. The degenerate form of Equation 5:

$$\frac{c_A}{c_A^s} = \frac{\phi}{\psi}(1 - \epsilon^{-\psi x}) \qquad c_A^o = 0$$

applies in the case where the inlet flow carries no species A. Note that Equation 5 applies to any arbitrary hydrodynamic flow regime. An alternative form of Equation 5 may be written as

$$\frac{c_A}{c_A^o} = \epsilon^{-\psi(r)x} + \beta(1 - \epsilon^{-\psi(r)x}) \qquad (6)$$

since β is independent of the flow regime.

The performance of the reactor may be characterized by two figures of merit:

$$\text{(A)} \qquad \frac{\hat{c}_A}{c_A^o} = \frac{2}{R^2 c_A^o}\int_0^R r c_A \, dr \qquad (7a)$$

yielding the horizontal sectional average of the concentration of species A, and specifically, at the reactor exit plane at $x = L$, and

$$\text{(B)} \qquad \frac{\bar{c}_A}{c_A^o} = \frac{2}{R^2 L c_A^o}\int_0^R \int_0^L r c_A \, dx \, dr \qquad (7b)$$

yielding the average concentration in the reactor.

2.2. *Application to plug-flow and parabolic-flow models of reactors*

The plug-flow model postulates a constant velocity in a reactor, whereas the parabolic flow model sets a parabolic transversal velocity distribution

$$u = 2u_m[1 - (r/R)^2] \qquad (8)$$

Both models have been used extensively in the literature to approximate real-reactor flow patterns. If parabolic flow is assumed, the figures of merit may be written as

$$\frac{\hat{c}_A}{c_A^o} = \beta + \frac{2(1-\beta)}{R^2}\int_0^R \epsilon^{-\psi(r)x} r \, dr \qquad (9a)$$

and

$$\frac{\bar{c}_A}{c_A^o} = \beta + \frac{2(1-\beta)}{R^2}\int_0^R \frac{1 - \epsilon^{-\psi(r)L}}{\psi(r)L} r \, dr \qquad (9b)$$

When $c_A^o = 0$, the equations simplify to

$$\frac{\hat{c}_A}{c_A^s} = \frac{2}{R^2} \cdot \frac{a_\phi}{a_\psi} \int_0^R [1 - \epsilon^{-\psi(r)x}] r \, dr \qquad (9c)$$

and

$$\frac{\bar{c}_A}{c_A^s} = \frac{a_\phi}{a_\psi} \left[1 - \frac{2}{R^2} \int_0^R \frac{1 - \epsilon^{-\psi(r)L}}{\psi(r)L} r \, dr \right] \qquad (9d)$$

with parameters

$$\phi \equiv \frac{a_\phi}{R^2 + r^2} \text{ and } \psi \equiv \frac{a_\psi}{R^2 + r^2} \qquad (9e)$$

representing the radial dependence; in the plug-flow model ϕ and ψ are constants and the integration procedure in Equation 9 is simplified.

3. Analysis

3.1. *The effect of residence time on performance*

If L, k_1 and c_A^o are constant, and the residence time is large, i.e. the linear velocity is small, there is sufficient time available for species A to reach the bulk solution via mass transport from the electrode. Unless the specific rate of its chemical decomposition is large relative to the mass transport rate it may, therefore, be expected that the smaller u, the larger the c_A/c_A^s ratio. If, conversely, the residence time is small, the supply of c_A to the bulk from the electrode surface is insufficient to counteract the effect of its chemical decomposition: the larger u, the smaller the c_A/c_A^s ratio. Its numerical value will be governed, of course, by k_1 and c_A^o, in addition to mass transport. The qualitative behaviour of the reactor with a parabolic-flow profile can be interpreted as essentially a 'superposition' of the plug-flow case at increasingly smaller linear velocities from centre-line to wall. All other parameters being constant, the c_A/c_A^s ratio becomes progressively smaller from wall to centre-line, since u increases with decreasing r and it reaches its lowest value at the centre line where the linear velocity is largest. The numerical values of k_1 and c_A^o are additional factors to determine the numerical values of c_A/c_A^s, as in the case of the plug-flow regime.

3.2. *Critical operating conditions*

A segment of the reactor operates under critical conditions, if the rate of supply and the rate of renewal of species A are exactly matched in the segment. The conditions of critical operation are given by

$$\left(\frac{c_A^s}{c_A^o}\right)_{cr} = \frac{\psi(r_{cr})}{\phi(r_{cr})} \qquad \text{(parabolic-flow)} \qquad (10a)$$

$$\left(\frac{c_A^s}{c_A^o}\right)_{cr} \equiv \frac{\psi}{\phi} = 1 + \frac{A_c k_1}{a k_m} \qquad \text{(plug flow)} \qquad (10b)$$

and $\beta = 1$. If species A is the desired product (whose chemical decomposition is undesired, but unavoidable), the reactor must be operated above the critical fractional surface concentration. If species A is an undesired intermediate whose decomposition is required e.g. for pollution control, the reactor must be operated under the critical value. Equation 10 holds only approximately if the surface concentration varies along the axial coordinate.

3.3. *The effect of flow regime on reactor length, at a specified extent of decomposition*

In principle, a plug-flow reactor is more efficient than reactors with velocity distributions. Thus, if c_A/c_A^o is set as a design postulate, a reactor with parabolic velocity distribution must have a larger active length than if it were a plug-flow reactor. The ratio of the active lengths pertaining to the two models can be determined readily, as shown below.

3.4. *Numerical illustration*

For the sake of numerical demonstration, earlier

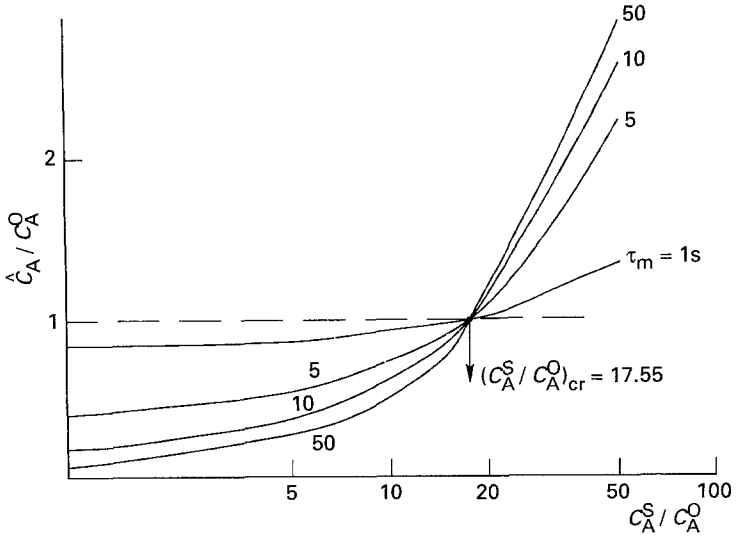

Fig. 1. The effect of the c_A^s/c_A^o ratio on the fractional exit concentration in parabolic flow, at various mean residence times in the numerical illustration.

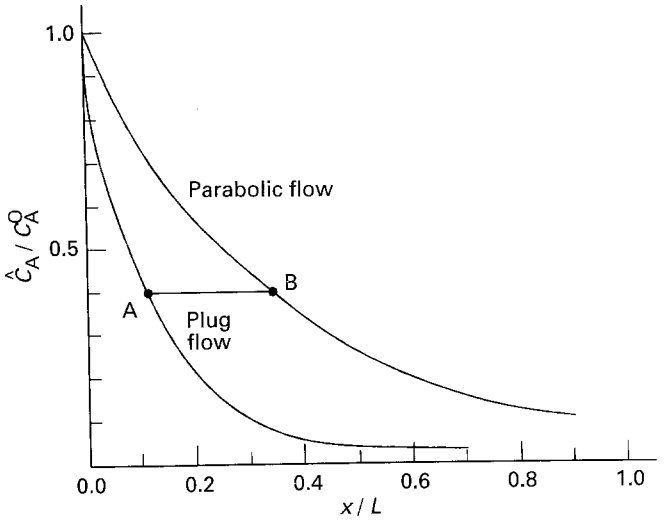

Fig. 2. The effect of the flow regime on electrolyser performance in the numerical illustration. $c_A^s/c_A^o = 1/2$; $\tau_m = 40$ s.

Table 1. Parameters of the electrochemical reactor in the numerical illustration

Parameter and its unit	*Numerical value*
Electrode area per unit length, a ($cm^2\,cm^{-1}$)	145.0
Active cross sectional area, A_c(cm^2)	180.0
Mean mass transfer coefficient, k_m($cm\,s^{-1}$)	0.015
Specific rate of the chemical decomposition reaction, k_1(s^{-1})	0.20
ψL (plug flow) τ_m unit : s	$0.2121\tau_m$
$\psi(r)L$ (parabolic flow) τ_m unit : s	$\dfrac{6.075}{57.29 + r^2}$
ϕ/ψ (plug flow) $\phi(r)/\psi(r)$ (parabolic flow)	0.057

research on DPA decomposition [29–32] was employed as a reference-guide for the choice of the prime operating parameters, assembled in Table 1. The variation of the normalized exit concentration with the normalized electrode surface concentration is shown in Fig. 1 in terms of parametric curves of the mean residence time; the critical $(c_A^s/c_A^o)_{cr} = 17.55$ ratio divides the concentration domain into two subdomains. Below the critical value the inlet concentration of species A is sufficiently large (with respect to c_A^s) to result in larger decomposition at larger residence times. Above the critical value c_A^s is sufficiently large (with respect to c_A^o) to supply larger amounts of species A to the bulk at larger residence times, hence conversion of species A to its decomposition product becomes smaller. At the critical point, there is no conversion, regardless of the value of c_A^s/c_A^o and the reactor becomes nonoperational.

Figure 2 illustrates the flow regime effect on performance. If, for instance the design postulate is $\hat{c}_A/c_A^o = 0.4$ (or 60% overall conversion) at $c_A^s/c_A^o = 1/2$ and $t_m = 40$ s, a reactor whose hydrodynamic behaviour may be approximated by parabolic flow, will have to have an effective length $B/A = 0.34/0.11 \cong 3.1$ times larger than in the case of plug-flow hydrodynamics.

4. Conclusion

Although the analysis is limited to plug-flow and parabolic-flow based hydrodynamics in the electrolytic reactor, the fundamental framework of analysis can entertain, in principle, any velocity distribution of a known mathematical form: specifically, Equations 2–5 and 7 apply without restriction to any arbitrary velocity profile. Since plug-flow and parabolic-flow represent two extreme regimes, the approach applied to an electrolyser with arbitrary hydrodynamics will yield the lower and upper bounds of performance. In electrolyser design, it can prove useful as a tool in a preliminary simulation of system behaviour.

Acknowledgements

This, and similar research, has been supported by the Natural Sciences and Engineering Research Council of Canada. Computations were performed on equipment supplied under a research agreement between the Digital Equipment Corporation and the University of Waterloo, Ontario.

References

[1] M. D. Hawley, Electrochemical evaluation of the mechanisms of organic reactions through examples, *in* 'Laboratory Techniques in Electroanalytical Chemistry', (edited by P. T. Kissinger and W. R. Heineman), Marcel Dekker New York (1984) Chapter 17.
[2] M. Baizer, 'Organic Electrochemistry', Marcel Dekker New York (1973).
[3] S. Swann Jr and R. Alkire, 'Bibliography of Electro-Organic Syntheses 1801-1975', The Electrochemical Society, Port City Press, Baltimore, MD (1980).
[4] M. R. Rifi and F. H. Covitz, 'Introduction to Organic Electrochemistry', Marcel Dekker New York (1974).
[5] J. E. Nolan and J. A. Plambeck, *J. Electroanal. Chem.* **286** (1990) 1.
[6] *Idem, ibid.* **294** (1990) 1.

[7] J. M. Savéant and E. Vianello, *Electrochim. Acta* **12** (1967) 629, 1545.
[8] C. P. Andrieux, L. Nadjo and J. M. Savéant, *J. Electroanal. Chem.* **26** (1970) 147.
[9] M. L. Olmstead, R. G. Hamilton and R. S. Nicholson, *Anal. Chem.* **41** (1969) 260.
[10] M. S. Shuman, *ibid.* **42** (1970) 521.
[11] D. H. Evans, *J. Phys. Chem.* **76** (1972) 1160.
[12] J. M. Savéant, *Electrochim. Acta* **12** (1967) 999.
[13] C. Amatore, J. Pinson and J. M. Savéant, *J. Electroanal. Chem.* **137** (1982) 143.
[14] J. M. Savéant, *Acta Chem. Scand. Ser.* **B37** (1983) 365.
[15] A. Kapturkiewicz and M. K. Kalinowski, *J. Phys. Chem.* **83** (1978) 1141.
[16] R. E. Sioda, B. Terem, J. H. P. Utley and B. C. L. Weedon, *J. Chem. Soc. Perkin I* (1976) 561.
[17] Z. Chami, M. Gareil, J. Pinson, J. M. Savéant and A. Thiebault, *J. Org. Chem.* **56** (1991) 586.
[18] K. M. Yin, T. Yen and R. E. White, *J. Electrochem. Soc.* **138** (1991) 1051.
[19] D. W. Wipf, E. W. Kristensen, M. R. Deakin and R. M. Wightman, *Anal. Chem.* **60** (1988) 306.
[20] C. A. Amatore, A. Jutland and F. Plunger, *J. Electroanal. Chem.* **281** (1987) 361.
[21] C. Lamonieux, C. Moinet and A. Tallec, *J. Appl. Electrochem.* **16** (1986) 819.
[22] R. E. Sioda, *Electrochim. Acta* **20** (1975) 457.
[23] R. L. C. Bosworth, *Phil. Mag. Series A* **39** (1948) 847.
[24] R. E. Sioda, *Analyst* **113** (1988) 489.
[25] R. E. Sioda and D. J. Curran, *J. Electroanal. Chem.* **239** (1988) 1.
[26] R. E. Sioda and T. Z. Fahidy, *J. Appl. Electrochem.* **18** (1988) 853.
[27] N. Winograd and T. Kuwana, *J. Am. Chem. Soc.* **92** (1970) 224.
[28] J. W. Strojek, T. Kuwana and S. W. Felberg, *ibid.* **90** (1968) 1353.
[29] R. C. Alkire and R. M. Gould, *J. Electrochem. Soc.* **127** (1980) 605.
[30] R. E. Sioda, *J. Phys. Chem.* **72** (1968) 2322.
[31] K. Scott, 'Electrochemical Reaction Engineering', Academic Press London (1991) Section 3.2.
[32] D. T. Chin and C. Y. Cheng, Electrochemical engineering principles as related to electroorganic processes, *in* 'Technique of Electroorganic Synthesis', Part III (edited by N. L. Weinberg and B. V. Tilak) Wiley, New York (1982) Chapter 1.